# Contents - A through D

# Measurements of Photoelectric Yield and Physical Properties of Individual Lunar Dust Grains

M. M. Abbas[1], D. Tankosic[2,] P. D. Craven[1], J. F. Spann[1], A. LeClair[2], E. A. West[1], L. Taylor[3], and R. Hoover[1]
[1] NASA-Marshall Space Flight Center, Huntsville, AL 35812
[2]University of Alabama in Huntsville, Huntsville, AL 35899
[3]University of Tennessee, Knoxville, TN, 37996

## ABSTRACT

Micron size dust grains levitated and transported on the lunar surface constitute a major problem for the robotic and human habitat missions for the Moon. It is well known since the Apollo missions that the lunar surface is covered with a thick layer of micron/sub-micron size dust grains. Transient dust clouds over the lunar horizon were observed by experiments during the Apollo 17 mission. Theoretical models suggest that the dust grains on the lunar surface are charged by the solar UV radiation as well as the solar wind. Even without any physical activity, the dust grains are levitated by electrostatic fields and transported away from the surface in the near vacuum environment of the Moon. The current dust charging and the levitation models, however, do not fully explain the observed phenomena. Since the abundance of dust on the Moon's surface with its observed adhesive characteristics is believed to have a severe impact on the human habitat and the lifetime and operations of a variety of equipment, it is necessary to investigate the phenomena and the charging properties of the lunar dust in order to develop appropriate mitigating strategies.

We will present results of some recent laboratory experiments on individual micron/sub-micron size dust grains levitated in electrodynamic balance in simulated space environments. The experiments involve photoelectric emission measurements of individual micron size lunar dust grains illuminated with UV radiation in the 120-160 nm wavelength range. The photoelectric yields are required to determine the charging properties of lunar dust illuminated by solar UV radiation. We will present some recent results of laboratory measurement of the photoelectric yields and the physical properties of individual micron size dust grains from the Apollo and Luna-24 sample returns as well as the JSC-1 lunar simulants.

**DUST PROPERTIES IN THE TRAIL OF COMET 67P/CHURYUMOV-GERASIMENKO.** J. Agarwal[1], H. Boehnhardt[2], M. Mueller[3] and E. T. Gruen[1,4]. [1]MPI-K, Saupfercheckweg 1, 69117 Heidelberg, Germany, jessica.agarwal@mpi-hd.mpg.de; [2]MPS, Max-Planck-Straße 2, 37191 Katlenburg-Lindau, Germany; [3]EDS at ESA/ESOC, Robert-Bosch-Str. 5, 64293 Darmstadt, Germany; [4]HIGP, University of Hawaii, 1680 East West Road POST 512c, Honolulu, HI 96822, USA.

**Introduction:** We report first results concerning the dust abundance and size distribution in the trail of comet 67P/Churyumov-Gerasimenko. The study is based on optical imaging data obtained in April 2004 with the Wide Field Imager (WFI) at the MPG/ESO 2.2m telescope in La Silla (Chile). For comparison we simulate images using a model with parameters derived from the observed emission history of the comet. By fitting the simulated intensity distribution to the observed one, we infer on the dust size distribution and column density. 67P/Churyumov-Gerasimenko is the target of ESA's Rosetta mission which will pass through the trail region during its approach to the nucleus in 2013.

**Comet trails:** Large (mm-sized) dust particles are emitted by comets at small heliocentric distances and with low relative velocities (several m/s). Since the strength of solar radiation pressure is weak compared to the gravity of the Sun, such particles move on trajectories similar to that of their parent comet. They concentrate along its orbit and appear to the observer as a long, line-shaped structure, the comet's dust trail. The emission of large dust particles is the principal mechanism by which a comet loses refractory mass to the interplanetary dust environment [1]. Trails of eight short-period comets were first observed with IRAS in 1983 [2,3], one of them being 67P/Churyumov-Gerasimenko.

**Trail imaging:** Comet trails are best observed when separated from smaller-sized dust grains. The latter are emitted with greater relative velocities and subject to stronger radiation pressure, hence they disperse in space on timescales of weeks to months from their release and their presence is not expected in the vicinity of an inactive comet far from the Sun. The WFI image (Fig. 1) was taken when 67P/Churyumov-Gerasimenko was at a heliocentric distance of 4.7 AU and we can confirm that no coma or young tail containing small particles is present in the image.

**Trail modelling:** We use a semi-analytical, generalised Finson-Probstein[4,5] model to produce simulated images of the dust trail [6]. For the time-dependent gas and dust production rates, we use observed values compiled from the literature, and the dust emission speed is computed using a hydrodynamic coma model [7]. The dust size distribution is the parameter we try to optimise by fitting the simulated image to the observed one. We find that using the size distribution derived in [8] from the VEGA2 measurements near comet 1P/Halley, is not optimal to reproduce the observed data and that a flatter size distribution is probably more appropriate.

**References:** [1] Sykes M.V. and Walker R.G. (1992) *Icarus, 95,* 180-210. [2] Sykes M.V. et al. (1986) *Science, 232,* 1115-1117. [3] Sykes M.V. et al. (1986) *Adv. Sp. Res., 6,* 67-78. [4] Finson M.L. and Probstein R.F. (1968a) *ApJ, 154,* 327-352. [5] Finson M.L. and Probstein R.F. (1968b) *ApJ, 154,* 353-380. [6] Agarwal J. et al. (2005) *Adv. Sp. Res, in press.* [7] Landgraf M. et al. (1999) *Planet. Space Sci., 47,* 1029-1050. [8] Divine N. and Newburn R.L. (1987) *A&A, 187,* 867-872.

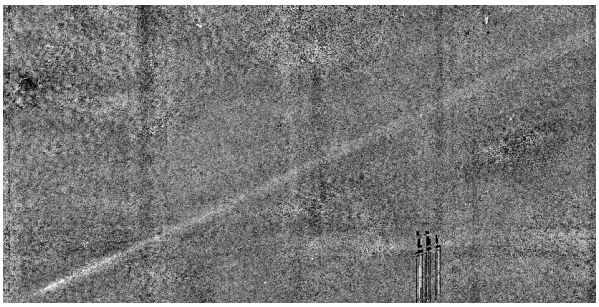

Fig. 1 - The trail of 67P/Churyumov-Gerasimenko in April 2004, observed with WFI at ESO/MPG 2.2m, La Silla. The image dimension corresponds to about 1 degree in mean anomaly and the nucleus is in the lower left corner, in the region which with the employed grey-scale range is saturated. The comet was at a heliocentric distance of 4.7 AU, and 3.7 AU from Earth.

**EXTREME OXYGEN ISOTOPE RATIOS IN METEORITIC DUST GRAINS — A RECORD OF IRRADIATION IN DUST-FORMING REGIONS OF THE PROTOSOLAR NEBULA?** Aléon J.[1,2], Duprat J.[3], Robert F.[4], Hutcheon I. D.[2], Weber, P. K.[2], Toppani A.[2] and Derenne S.[5]. [1]CRPG-CNRS, 15 rue Notre Dame des Pauvres, 54501 Vandoeuvre-les-Nancy, France (aleon@crpg.cnrs-nancy.fr), [2]LLNL, Livermore, CA 94550, USA, [3]CSNSM, Bat 104, 91405 Orsay campus, France, [4]LEME-MNHN, 61 rue Buffon 75005 Paris, France, [5]LCBOP-ENSCP, 11 rue Pierre et Marie Curie 75231 Paris, France.

**Introduction:** Large isotopic anomalies in minute meteoritic and cometary grains are commonly attributed to the survival of interstellar dust grains formed in previous generations of stars [1]. In this study, we mapped large oxygen isotope anomalies associated with unusual dust grains embedded in an organic residue from the carbonaceous chondrites Orgueil and Murchison.

**Samples and analytical techniques:** O isotopes were mapped at high mass resolving power by IMS 1270 ion microprobe at CRPG, Nancy using a 1 µm lateral resolution in insoluble organic matter from Orgueil and Murchison. Grains with isotopic anomalies were subsequently mapped for Si isotopes with 2 µm lateral resolution to increase the sensitivity and anlayzed by scanning electron microscopy (SEM). Residual grains were selected for (1) Mg isotope analysis by NanoSIMS at Lawrence Livermore National Laboratory (LLNL) with 200 nm lateral resolution, (2) N isotope analysis by IMS 1270 ion microprobe in CRPG, Nancy with 1 µm lateral resolution and (3) focussed ion beam sectioning followed by transmission electron microscopy (TEM) performed at LLNL.

**Results**: 36 grains with large excesses of $^{17}O$ and $^{18}O$ were discovered in the IOM from Murchison, while none were found in IOM from Orgueil. $^{17}O/^{16}O$ and $^{18}O/^{16}O$ ratios of these grains reach the largest values ever measured in solar system materials : $7.7 \times 10^{-2}$ and $1.2 \times 10^{-1}$, respectively. By contrast with typical presolar grains which show the scatter expected from the contribution of multiple stellar sources, all Murchison grains lie on a single mixing line between the most extreme value and the bulk solar system value [2]. Given the yield of IOM extraction and the relative surface area analyzed, the grains account for ~1 ppm of Murchison, a concentration comparable with that of presolar oxide grains [1]. The abundance of similar grains is less than 40 ppb in Orgueil. In contrast to O, no deviations from solar system values were found for N, Mg or Si (uncertainties: 10 ‰ on Si isotopes, 20 ‰ on Mg isotopes, a factor 2 on N isotopes). The upper limit on the initial $^{26}Al/^{27}Al$ inferred from Mg isotopes is $4.8 \times 10^{-4}$. SEM imaging and energy dispersive spectroscopy revealed that the grains are facetted with Si and O being the only major constituents, suggesting that the grains could be silica. Preliminary TEM results suggest that the grains are amorphous silica.

**Discussion:** Large excesses of both $^{17}O$ and $^{18}O$ associated with normal Si and Mg isotopic compositions cannot be explained by conventional stellar nucleosynthesis models. Similar O isotopic ratios have been observed only once in our galaxy, in HR4049, an unusual post-asymptotic giant branch star [3]. If the Murchison grains originated in such a star, the fact that all O-isotope values lie along a single mixing line indicates the young solar system may have encountered a single unusual star responsible for the injection of these grains. However we note that this hypothesis is in contradiction with (1) the absence of anomalous grains in Orgueil, a meteorite rich in presolar grains, (2) the absence of large amounts of $^{26}Al$ in the grains, and (3) the absence of refractory oxide grains with similar compositions [1].

The observed compositions are successfully reproduced by irradiating a gas of solar composition by particles with the characteristics of $^{3}He$-rich impulsive solar flares, followed by condensation and selective chemical trapping of anomalous O (O*). Such a condensation reaction could be $SiO + O^* \rightarrow SiO_2$. In this model the absence of Si isotope anomalies is explained by the dilution in the solar gas of the intermediate species, SiO. This may also be the case for Mg and Al. Any species trapped mechanically in the grains, such as the inert gas $N_2$, would also have the composition of the bulk solar gas. We propose that the isolation of O* followed by condensation could have taken place in energetic protosolar outflows. Protostellar outflows are commonly enriched in SiO [4], possibly allowing condensation of $SiO_2$. The discovery of these grains thus suggests that large isotopic anomalies could be produced within the young solar system and record highly energetic processes during an active phase of the young Sun.

**References:** [1] Clayton D.D. and Nittler L.R. (2004) *ARAA* 42, 39-78. [2] Aléon J. et al. (2005) *Nature* in press. [3] Cami J. and Yamamura I. (2001) *A&A* 367, L1-L4. [4] Nisini B. et al. (2002) *A&A* 395, L25-L28.

# In-Situ Spacecraft Monitoring of the Interstellar Dust Stream in the Inner Solar System

N. Altobelli[1], E.Grün[2], S.Kempf[3], H.Krüger[4], M.Landgraf[5], R.Srama[6]

[1] NASA/JPL 4800 Oak Grove Drive CA-91101 Pasadena USA, nicolas.altobelli@jpl.nasa.gov, [2] MPIK, Saupfercheckweg 1, 69117 Heidelberg, Germany/HIGP, University of Hawaii, Honolulu, USA, Eberhard.gruen@mpi-hd.mpg.de [3] MPIK, Saupfercheckweg 1, 69117 Heidelberg, Germany, sascha.kempf@mpi-hd.mpg.de [4] MPS, 37191 Katlenburg-Lindau, Germany, krueger@mps.mpg.de [5] ESA/ESOC, 64293 Darmstadt, Germany, markus.landgraf@esa.int [6] MPIK, Saupfercheckweg 1, 69117 Heidelberg, Germany, ralf.srama@mpi-hd.mpg.de

The Solar System motion relative to the surrounding interstellar medium results in a wind of gas and dust particles blowing onto the boundary region of the heliosphere. Evidence was found in 1993 by the dust detector on-board the *Ulysses* spacecraft that a collimated stream of interstellar dust (ISD) grains on hyperbolic trajectory penetrates deeply into the Solar System [Grün et al., 1993]. The downstream flux direction is compatible with the interstellar helium flux [Baguhl et al., 1995] and the bulk of its mass distribution is around $10^{-16}$kg [Landgraf et al., 2000]. In-situ observation of ISD grains is of strong astrophysical interest and allows us to retrieve crucial information on individual grains which is not accessible by astronomical observations.

Over the past decade, study of the ISD flux alteration under the influence of the heliospheric environment provided important clues to the physical properties of individual ISD grains. Dynamics of ISD grains is ruled mainly by three perturbating accelerations: the Sun's gravitation (involving the grain mass), the radiation pressure (involving the grain's surface optical properties) and the Lorenz perturbation resulting from the coupling of charged grains (according to their charge-to-mass ratio) with the interplanetary magnetic field (IMF). The relative strength of these perturbations is also dependent upon the location in the Solar System and is reflected by the ISD flux alteration. Therefore, to better constrain the grain properties, it is highly desirable to determine the ISD flux value at many different locations in the Solar System. The *Ulysses* spacecraft measurements were performed between 2.5 and 5 AU. We analyze dust data sets retrieved by the interplanetary probes *Helios*, *Galileo*, and *Cassini*, extending the heliocentric distance range of the ISD observations down to 0.3 AU.

The ISD data presented here have been obtained on orbit segments where a discrimination between ISD and the interplanetary dust particles (IDPs) background was possible. The identification scheme used for this analysis involves geometrical criteria and criteria based on the comparison of the impact energy. A careful selection of the orbit segments is required: the impact energy of ISD grains is higher when the spacecraft is moving toward the ISD downstream direction, while the impact energy of IDPs on bound orbit is constrained by their orbital elements and mass distribution, evaluated from an interplanetary dust flux model.

We first applied our identification scheme to the *Cassini* dust data during the interplanetary cruise phase when the spacecraft was located between Venus and the Earth. An ISD flux of about $2.5 \cdot 10^{-5} \mathrm{m}^{-2}\mathrm{s}^{-1}$ was detected. The energy of the ISD impactors was compatible with typical grain masses of about $3 \cdot 10^{-16}$ kg, as derived from the analysis of the *Ulysses* ISD data [Landgraf et al., 2000]. The analysis of the *Galileo* data between the orbits of Venus and Mars confirmed the presence of ISD at close heliocentric distances. About 115 ISD impactors were identified amongst 435 dust impact events between December 31st, 1989 and December 31st, 1993. Finally, the *Helios* dust data (235 impactors) obtained between December 1974 and January, 1980 were also analyzed for ISD. A weak but significant ISD flux of about $2.6 \pm 0.3 \cdot 10^{-6}$ $\mathrm{m}^{-2}\mathrm{s}^{-1}$ was detected down to 0.3 AU (see Fig. 1). Interestingly, the *Helios* ISD data suggest larger grains (micrometer size) than detected with the other instruments (sub-micrometer size).

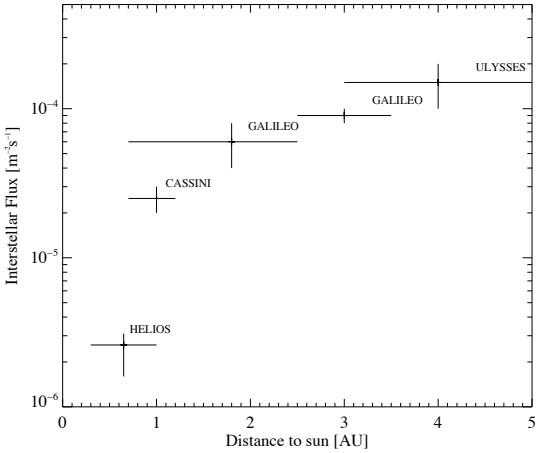


Figure 1: Plot showing the values of the ISD flux calculated with the data presented in this work, as function of the heliocentric distance.

The decrease of the ISD flux at close heliocentric distances can be explained by the radiation pressure filtering effect. Zones of avoidance are shaped by the solar radiation, inside which ISD grains smaller than a certain size can not penetrate [Landgraf, 2000]. Our ISD flux measurements show a good agreement with the theoretical boundary locations of the avoidance zones, assuming for the dust grain surface optical properties the astronomical silicates model [Gustafson, 1994]. On the other hand, the spatial density of big ISD grains is enhanced by gravitation focusing at close heliocentric distances. Thus, the closer to the Sun, the bigger the low-mass cut off of ISD grains. This picture is supported by the excess of big ISD grains found in the *Helios* ISD data.

Furthermore, clues to the elemental composition of the ISD grains detected were found by the *Helios* time-of-flight mass spectrometer, indicating that individual grains are a varying mixture of various mineral and carbonaceous compounds.

## References

[Baguhl et al., 1995] Baguhl, M., Grün, E., Hamilton, D. P., Linkert, G., Riemann, R., and Staubach, P. (1995). The flux of interstellar dust observed by Ulysses and Galileo. *Space Sci. Rev.*, 72:471–476.

[Grün et al., 1993] Grün, E., Zook, H., Baguhl, M., Balogh, A., Bame, S., Fechtig, H., Forsyth, R., Hanner, M., Horanyi, M., Kissel, J., Lindblad, B.-A., Linkert, D., Linkert, G., Mann, I., McDonnel, J., Morfill, G., Phillips, J., Polanskey, C., Schwehm, G., Siddique, N., Staubach, P., Svestka, J., and Taylor, A. (1993). Discovery of Jovian dust streams and interstellar grains by the Ulysses spacecraft. *Nature*, 362:428–430.

[Gustafson, 1994] Gustafson, B. (1994). Physics of zodiacal dust. *Ann. Rev. Earth Planet. Sci.*, 22:553–595.

[Landgraf, 2000] Landgraf, M. (2000). Modeling the motion and distribution of interstellar dust inside the heliosphere. *J. Geophys. Res.*, 105:10303–10316.

[Landgraf et al., 2000] Landgraf, M., Baggaley, W. J., Grün, E., Krüger, H., and Linkert, G. (2000). Aspects of the mass distribution of interstellar dust grains in the solar system from in situ measurements. *J. Geophys. Res.*, 105:10343–10352.

**Interplanetary dust between Jupiter and Saturn: preliminary results from the Cassini Cosmic Dust Analyzer.** N. Altobelli (1) and M. Roy (2), S.Kempf (3), R.Srama (4), Georg Moragas-Klostermeier (5), E. Grün (6). (1)NASA/JPL 4800 Oak Grove Drive CA-91101 Pasadena USA nicolas.altobelli@jpl.nasa.gov, (2)NASA/JPL 4800 Oak Grove Drive CA-91101 Pasadena USA mou.roy@jpl.nasa.gov, (3)MPIK, Saupfercheckweg 1, 69117 Heidelberg, Germany sascha.kempf@mpi-hd.mpg.de, (4) MPIK, Saupfercheckweg 1, 69117 Heidelberg, Germany ralf.srama@mpi-hd.mpg.de, (5)MPIK, Saupfercheckweg 1, 69117 Heidelberg, Germany moragas@mpi-hd.mpg.de, (6) MPIK, Saupfercheckweg 1, 69117 Heidelberg, Germany/ HIGP university of Hawaii, Honolulu, USA eberhard.gruen@mpi-hd.mpg.de.

**Introduction:** We report in this work the preliminary analysis of the Cosmic Dust Analyzer (CDA) data, obtained when the Cassini spacecraft was between Jupiter and Saturn. The data cover the time period between the Jupiter fly-by and the Saturn orbit insertion (SOI).

**Previous analysis:** Until the Cassini mission, the only in situ dust detectors ever flown in this region were the Pioneer 10 and Pioneer 11 dust experiments. A nearly constant flux of interplanetary dust (IDP) about 10^-6/m^2/s was derived from the Pioneer instruments data outside the orbit of Jupiter [2]. Owing to the sensitivity of these instruments, only big particles (larger than 10 μm for Pioneer 10 and larger than 25 μm for Pioneer 11) could be detected. Three dust sources accounting for the measured flux beyond 5 AU were identified, involving short-period Oort cloud comets (retrograde particles with low inclination), short-period Jupiter-family comets (low eccentricities and inclinations) and Edgeworth-Kuiper belt objects (low eccentricities and inclinations) [4].

**Preliminary results and goals of this work:** The CDA is a more sensitive instruments and allows the detection of smaller grains. In particular, streams of high-velocity submicrometre-sized dust particles, originating from both Jupiter and Saturn [1,3] are detected far away from their source and contribute significantly to the data set. However, bigger IDPs on bound low-inclined orbits have been detected as well. A preliminary analysis suggests both prograde and retrograde trajectories for these grains. As Cassini was located downstream to the interstellar dust (ISD) flux, no ISD grains can be detected on this part of the Cassini trajectory since this would require the instrument pointing to be directed toward the Sun (forbidden configuration). The IDP flux values measured are compared with the values derived from the Pioneer IDP data. Furthermore, deriving the flux value in the vicinity of Saturn provides a lower estimate of the IDP contamination onto the Saturn dust rings.

**References:**

[1] Grün, E., Zook, H., Baguhl, M., Balogh, A., Bame, S., Fechtig, H., Forsyth R., Hanner, M., Horanyi, M., Kissel, J., Lindblad, B.-A., Linkert, D., Linkert, G., Mann, I., McDonnel, J., Morfill, G., Phillips, J., Polanskey, C., Schwehm, G., Siddique, N., Staubach, P., Svestka, J., and Taylor, A. (1993). *Discovery of Jovian dust streams and interstellar grains by the Ulysses spacecraft.* Nature 362, 428-430.

[2] Humes, D.~H. (1980). *Results of Pioneer 10 and 11 meteoroid experiments – Interplanetary and near-Saturn.* JGR 85, 5841-5852.

[3] Kempf, S., Srama, R., Horanyi, M., Burton, M., Helfert, S., Moragas-Klostermeyer, G., Roy, M., and Grün, E. (2005). *High-velocity streams of dust originating from Saturn.* Nature 433, 289-291.

[4] Landgraf, M., Liou, J.-C., Zook, H.~A., and Grün, E. (2002). *Origins of Solar System Dust beyond Jupiter.* Astron. Journal 123, 2857-2861.

**DUST PRODUCTION DURING PLANETARY COLLISIONS LARGE AND SMALL.** E. Asphaug, C. Agnor and Q. Williams, IGPP Center for Origin, Dynamics & Evolution of Planets, Earth Sciences Dept. University of California, Santa Cruz CA 95064, asphaug@pmc.ucsc.edu

**Introduction:** Dust production in planetary systems has often been proposed to be the result of high strain rate fragmentation events, as asteroids and comets grind one another down to smaller and smaller sizes. But it is also possible to produce copious dust, particularly in young planetary systems, through pressure-release phreatic eruptions, as large planetary embryos rip each other to shreds, unloading 100's of kbars of pressure during late stage accretion.

Having recently demonstrated that planetary collisions are seldom accretionary [1; see Fig. 1], we find that disruptive tides and gravitational torques may do much of the work of planetary evolution. The focus here is predominantly upon the smaller of the encountering bodies – the "impactor" – which is frequently *not* accreted in a collision, and whose material is severely disrupted and in many cases pulled off of its central body (see Fig. 2), in events not dissimilar from the tidal break-up of comet Shoemaker-Levy 9. These planet-scale volumes of unloaded material are proposed as copious sources for dust production in early planetary systems. The character of this dust is predicted to be volcanic in origin and highly outgassed.

**Meteoritics and Impacts:** Impacts are typically understood as shock-related phenomena, based on laboratory comparison and our understanding of impact cratering. But shock physics fares poorly, in many instances, in explaining asteroid and meteorite genesis. Mixing by shock acceleration should leave few un-shocked products. Melting and thermal processing by impact are inefficient on small bodies [2] since material shocked to high temperature escapes their weak gravity. Melts, melt residues, welded agglomerates and hydrous and gas-rich phases are abundant among meteorites, leading to an array of diverse puzzles. Also puzzling is the relative abundance of stony-irons [~2-3% of all falls), when unambiguous mantle meteorites are rare [reviewed in 3 and refs therein]. Where are these mantle rocks, when so many irons and stony-irons were excavated from the deepest mantles and cores?

A possible solution is that mantle rock, when ripped from a parent planet, becomes dust in a single event related to gravitational unloading from hydrostatic equilibrium over the encounter timescale.

**Fragmentation by Elastic Unloading:** Consider a cold elastic planet, unloading by tidal stress during a gravitational timescale $\tau_{grav} \sim (G\rho)^{-1/2}$. If release rates are high, one can apply a dynamic fragmentation model [4] to evaluate the expected fragment size. Consider a Weibull distribution of active flaws per unit volume $n(\varepsilon) = k\varepsilon^m$, where $\varepsilon = \sigma/E$, $\sigma$ is the flaw activation stress, and $E$ the elastic modulus. Fragment size decreases with strain rate $\dot{\varepsilon}$. If the characteristic mantle stress $\sigma \approx G\rho^2 a^2$ unloads uniformly over $\tau_{grav}$, then the characteristic strain rate $\dot{\varepsilon} = G^{3/2}\rho^{5/2}a^2/E$ gives mean fragment size $L \approx 6 c_g \alpha^{-1/m+3} \dot{\varepsilon}^{-m/m+3}/(m+2)$, where $c_g$ is the crack growth velocity and $\alpha = 8\pi c_g^3 k/[(m+1)(m+2)(m+3)]$. Here $a$ is the disrupted body's radius. Fragment size decreases with almost the square of disrupted planet size, since $m$>~6 for most geologic materials. A 500 km diameter basalt sphere ($k$=4·10$^{29}$ cm$^{-3}$, $m$=9) cracks into ~200 m fragments if unloaded over $\tau_{grav}$, and a 1000 km sphere cracks into ~70 m fragments. Instant rubble piles result if these fragments do not disperse; families of sub-km asteroids form otherwise, thereafter comminuting to smaller sizes.

**Fragmentation During Viscous Response:** Viscous deformation is indicated when $\tau_{grav} < \tau_{maxwell}$, and this is the more likely scenario for accreting embryos where accretional heating and short half-life radionuclide decay kept them hot for millions of years. Viscosity decreases with $e^{-1/T}$, where $T$ is temperature. For power-law creep, $\dot{\varepsilon} = A\sigma^n$, about the

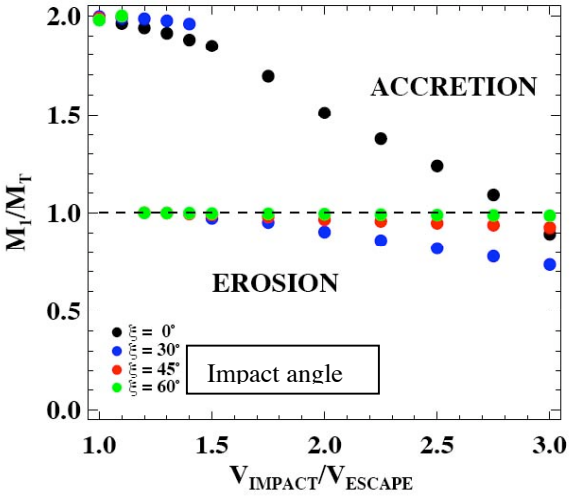


**Fig. 1** Many planetary collisions result in net mass loss, not mass accretion (from [1])

square of the applied stress ($n$~3 for cold ice and dry quartzite). As a guide, models of early-Earth convection assume mid-mantle viscosities ~$10^9$ poise [5], and η~$10^9$-$10^{13}$ poise is used [6] to model Io's present asthenosphere. Dissolved $H_2O$ expected in primitive mantles further lowers the viscosity, especially if exsolved during unloading (see below). Once tidal deformation begins, pressure unloading ensues, and this triggers partial melting and possible $H_2O$ exsolution, lowering the viscosity and leading to efficient melt segregation and possible outgassing.

Tidal disruption requires significant deformational strain, let's say $\varepsilon_{def} \approx 10$, accruing over a few times $\tau_{grav}$. The maximum viscosity $\eta_{\lim}$ allowing this deformation is approximately the stress that must be unloaded, $\sigma \approx G\rho^2 R^2$, divided by the required strain rate, $\dot{\varepsilon} \approx \varepsilon_{def} / \tau_{grav}$. This gives the result

$$\eta_{\lim} \approx \varepsilon_{def}^{-1} \sqrt{G} \rho^{3/2} a^2$$

Strains $\varepsilon_{def}$>10 can occur if $\eta < \eta_{\lim} \sim 10^{12} a_{km}^2$ poise (g cm$^{-1}$s$^{-1}$), where $a_{km} = a/(1000\text{ km})$.

Young planetary embryos are thus expected to be particularly vulnerable to viscous disruptive deformation. Once they cool, they still fail but by brittle fragmentation as described earlier, which as shown by Jeffreys will occur to grazing interlopers larger than about 200 km diameter [7].

These analyses describe mechanisms separately from impact shock, which further contributes to disruption, mass loss, and dust production.

**Gravitational Unloading:** A planet suffering a grazing (non-impacting) encounter at close to $v_{esc}$ with a planet ten times its mass unloads its interior pressure by about half. This unloading might trigger degassing and dust production as the material unloads from an existing high-pressure hydrostatic state. The energy per unit mass during decompression is $\int dP/\rho$, which for constant density (e.g. up to the onset of vaporization) is $\sim P/\rho \approx G\rho r^2 \sim 2 \cdot 10^{10}$ erg g$^{-1}$ for the base of a Mars-sized planet's mantle. The effect of this energetic release is very dependent on the equation of state. The fragments of comet Shoemaker-Levy 9 were very active, producing copious dust, probably owing to sudden exposure (large $dP$) of a pristine interior. A disrupted planetary embryo unloads from pressures millions of times greater, and if rich in mantle volatiles might erupt [e.g. 8].

**Mass Fractionation:** Without even touching the target, the planet above loses its outer mantle and crust, some in the form of a disk or satellite swarm. Impacting non-accretionary encounters have even more severe tidal effects, as will be discussed in the talk. The atmosphere is lost, as tidal deformation is greatest for the lowest density layers (demonstrated by the stretching-out of the dust-rich comae of comet SL9. Much of these outer materials drain down onto the larger planet, increasing the volatile and atmophile inventory of the larger body at the expense of the smaller. As tidal collisions are much more common than accretionary collisions, embryo volatile inventory will evolve to vary inversely with mass.

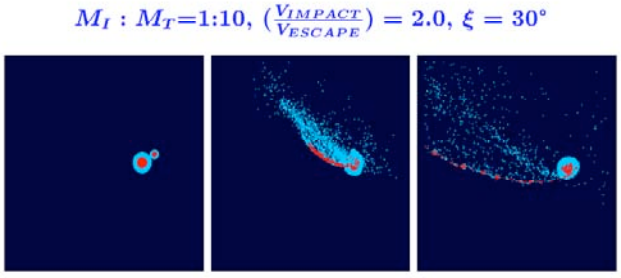


About half of impacts between planetary embryos in the late stage of accretion do not result in mass merger. What happens to the debris? (From [1])

**Degassing:** Extreme thermodynamical transitions raise the possibility of planetary degassing. The limited solubility of water in silicate liquids at low pressures can leave the shallow mantle of a primitive embryo relatively dry, down to a pressure of about 6 kbar, whereas deeper mantle can retain abundant water. As the planet unloads, the deep mantle crosses the water solubility pressure, so the question is whether there is adequate time for gas to segregate.

**Dust Production:** In the case of material stripped off of the host planet – in the manner of Shoemaker-Levy 9 but at much larger scales – the issue is less subtle. Transitioning from deep mantle pressures to almost complete unloading, over the course of hours, results in intense fragmentation, explosive degassing, and highly efficient dust production.

## REFERENCES

[1] Agnor, C. & Asphaug, E., Ap. J. 613, L157-L160 (2004).

[2] Keil, K. et al. MAPS 32, 349-363 (1997).

[3] Burbine, T. H., Meibom, A. & Binzel, R. P. (1996). Meteoritics 31, 607-620.

[4] Grady, D. E. & Kipp, M. E. (1980). Int. J. Rock Mech. Min. Sci. Geomech. Abstr. 17, 147-157.

[5] Walzer, U. et al.; Tectonophysics 384, 55-90..

[6] Tackley et al, Icarus 149, 79-93 (2001)

[7] Jeffreys, H. (1947). MNRAS 107, 260-272

[8] Wilson et al., MAPS 34, 541-557 (1999)

**DEVELOPMENT OF AN ULTRA-LOW NOISE CHARGE-SENSITIVE AMPLIFIER FOR COSMIC DUST PARTICLES**

S. Auer (dusty789@shentel.net)

A new amplifier is being developed for the Dust Trajectory Detector of the Dust Telescope project. It shall enable us to measure the trajectories of dust particles with charges as low as 10^-16C (600 electrons) with an accuracy of 1° in direction and 1% in speed. Particular emphasis is placed on new methods of resetting the amplifier to prevent its saturation when currents of solar wind electrons or of photoelectrons from are charging the sensing electrodes.

**COMPUTED ELECTRICAL CHARGES OF DUST PARTICLES WITH HIGHLY IRREGULAR SHAPES**

S. Auer (dusty789@shentel.net)

The electrical charges of highly irregular particles were computed. It turns out that long needles and snowflake-like particles assumed charges as high as 30 times the charge of a spherical particle having the same volume and surface potential. This ratio influences the derivation of a particle's mass from its charge.

**INTERSTELLAR METEORS.** W.J Baggaley, Physics and Astronomy Department, University of Canterbury, PB 4800, Christchurch, New Zealand. jack.baggaley@canterbury.ac.nz.

Interstellar dust particles larger than about 1μm ($4.10^{-12}$ g) can penetrate freely into the inner solar system where, in the event of Earth impact, they can be accessed by detecting the plasma and excited species created when the particles ablate in the Earth's atmosphere. The ablation process and current experimental techniques available for plasma detection mean that the particle size regime accessible from ground-based sensing is much larger than can be sampled from spacecraft. However, the much larger collecting area provided by the atmosphere in the meteor mode results in comparable detection statistics for the two techniques.

The value of this Earth based probing of interstellar dust lies in the ability to provide quality dynamical characteristics: the velocity information allows the tracking of pre-solar system encounter trajectories.

This paper provides an overview of experimental techniques and the attempts to map the galactic sources of interstellar dust.

**A REVOLUTION IN THE NANO-SCALE CHARACTERIZATION OF IDPs AND OTHER PRIMITIVE METEORITIC MATERIALS.** John P. Bradley, [1]Institute of Geophysics and Planetary Physics, Lawrence Livermore National Laboratory, Livermore CA , 94550 <jbradley@igpp.ucllnl.org>

**Introduction:** In the past five years a suite of new instruments have enabled materials scientists to significantly advance the state-of-the-art in the analysis of nano-materials. These instruments include the Focused Ion Beam (FIB), nanoSIMS and an emerging generation of analytical scanning transmission electron microscope known generically as the SuperSTEM. We are developing an integrated approach to the microanalysis of IDPs and meteorites, using FIB, SuperSTEM, (and nanoSIMS), with the goal of expanding the science yield that can be obtained from a single sample. FIB is a key bridging technology that enables production of samples that can be interchanged between FIB, nanoSIMS and STEM environments.

The FIB utilizes a gallium ion beam within an SEM environment to harvest electron transparent sections and site-specific samples with sub-micrometer-scale spatial resolution. The biggest impact of FIB in meteoritics has been the almost routine recovery of isotopically anomalous "hot spots" from ion microprobe mounts, precipitating a flood of highly specific new data about the mineralogy and even optical properties of presolar grains [e.g. 1-3].

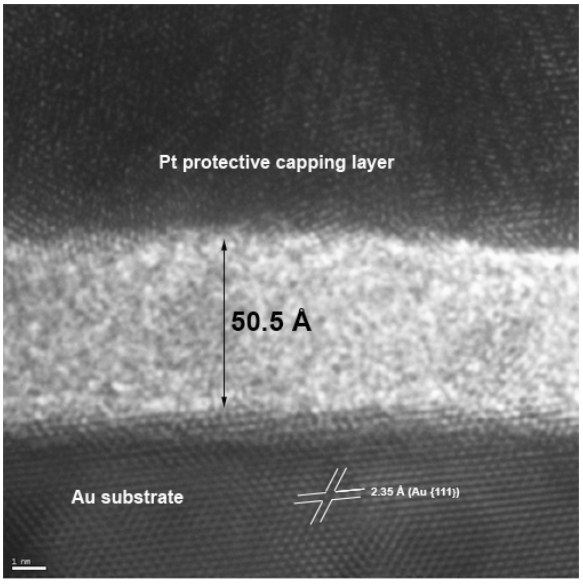


***Figure 1:*** *High-resolution lattice-fringe image of a solar-wind implanted Au substrate (lower) from the Genesis mission. The surface is coated with a contamination layer 50.5 Å thick. The Pt protective capping layer (upper) was applied during FIB specimen preparation. Scale bar measures 1 nm.*

FIB is proving useful in other critical areas of planetary materials analysis. Figure 1 shows a brightfield image of what is suspected to be a siloxane-based contaminant stain on the surface of a gold solar-wind collection substrate from the Genesis spacecraft. Measurements of the thickness of this layer using surface sensitive techniques yielded conflicting results ranging from 50 Å to 160 Å. Accurate measurement of the stain thickness may be a prerequisite to meaningful analyses of the isotopic compositions of the some of the implanted solar wind elements. Figure 1 establishes that the stain is 50 Å thick, at least in this region of the gold foil.

Significant new developments in analytical transmission electron microscopy include high-resolution electron energy-loss spectroscopy, optical spectroscopy and nanometer-scale compositional mapping. Figure 2 shows a 200 keV zero-loss peak obtained using a Tecnai™ F20 monochromated STEM recently installed at Lawrence Livermore National Laboratory (LLNL). The 0.07 eV energy resolution at a one second exposure is due to a higher stability high-voltage source, a monochromator and a high-resolution energy filter. This performance record for energy-loss spectroscopy opens a whole new level of chemical analysis at the nanometer scale by probing bonding states, bandgap and valence band

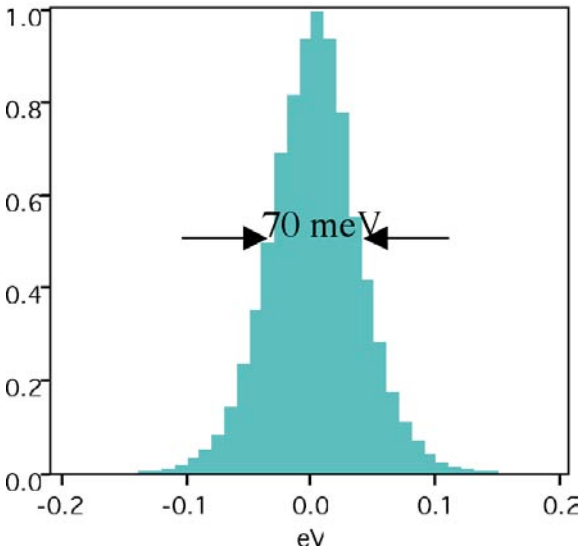


***Figure 2:*** *Electron energy-loss zero-loss peak obtained using a 200 keV monochromated transmission electron microscope.*

transitions of known and unknown materials. The overall spatial resolution is an order of magnitude better than synchrotron XANES and it is complimentary to that technique.

With improved energy resolution the width of the zero-loss peak is reduced, opening up a spectral region that contains a wealth of new information. For example, it is now possible to perform optical spectroscopy in the near-infrared, visible and UV spectral regions with nanometer-scale spatial resolution. Using this new capability, a spectral match to the astronomical 2175 Å extinction feature was recently observed within IDPs using EELS (Fig. 3) [4].

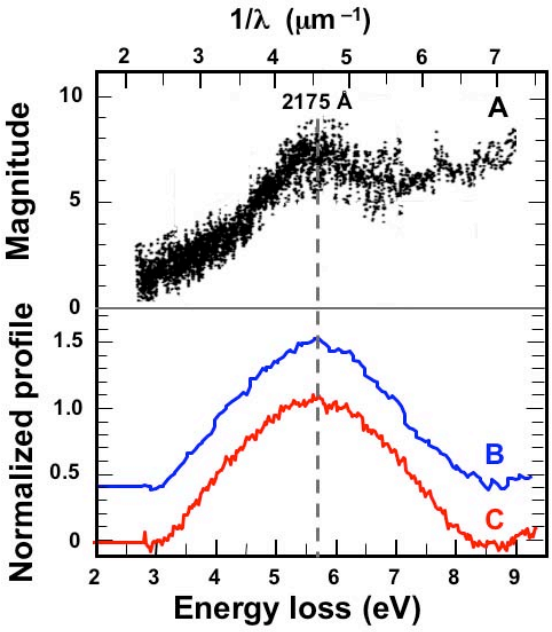


***Figure 3:*** *The astronomical 2175 Å UV extinction feature (A) compared with EELS UV spectra from IDPs (B & C). From Bradley et al., 2005* [4] *).*

Figure 4 shows the near-infrared, visible and UV region of an energy-loss spectrum of Acid Fuchsin obtained using the monochromated STEM at LLNL. (Acid Fuchsin is a common sodium salt histological stain used for staining cytoplasm and collagen). The spectrum was acquired using gun deceleration lens mode, a 1 mm spectrometer aperture, 0.01 eV/pixel dispersion and 1 second acquisition. Specimen thickness is 0.74x the inelastic mean free path. Zero-loss energy resolution is 0.18 eV FWHM on the specimen. The visible electron energy-loss absorption spectrum is due to electron optical transitions corresponding to exciting the molecular orbitals of the valence electrons, giving rise to the emission of photons in the visible region of the spectrum. A UV absorption peak at 5.9 eV (λ~210 nm) is clearly visible (as it is in the optical spectrum of Acid Fuchsin).

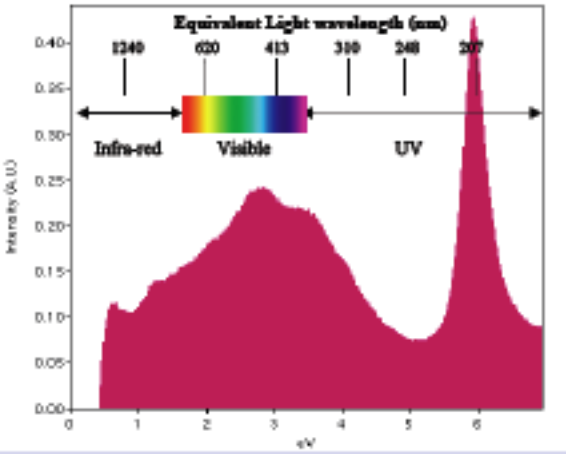


***Figure 4:*** *Near-infrared, visible and UV region of an energy-loss spectrum of Acid Fuchsin obtained using the monochromated STEM at LLNL (data courtesy of M.Barfels, (Gatan Inc) and Z. Dai (LLNL)).*

**References:** [1] Stroud R. M. and Bernatowicz T. J. (2005) *LPS XXXVI*, Abs# 2010. [2] Floss C. F. et al. (1997) *Meteoritics & Planet. Sci., 32*, A74. [3] Yada, T. et al., (2005) *LPS XXXVI*, Abs #1227. [4] Bradley J. P. et al. (2005) *Science 307*, 244-247.

**Acknowledgements:** This work was performed in part under the auspices of the U.S. Department of Energy, NNSA by the University of California and Lawrence Livermore National Laboratory under contract No. W-7405-Eng-48. This work was also performed as part of the Bay Area Particle Analysis Consortium (BayPAC). Supported by NASA grant NNH04AB491.

**INTERSTELLAR METEOROIDS DETECTED BY THE CANADIAN METEOR ORBIT RADAR**. P. Brown[1], R.J. Weryk[1], [1]Department of Physics and Astronomy, University of Western Ontario, London, ON, N6A 3K7

**Introduction:** The number density of very large (>50 μm) interstellar grains is largely unknown [1]. Such large interstellar particles (ISPs) are of interest as they could contain a significant mass fraction of the solids in interstellar space [2]. Larger grains also have their original trajectories less affected by Lorentz and gas drag forces in the interstellar medium in addition to having longer lifetimes against catastrophic collisions. As a result, it is more probable that the specific origin for a given large ISP (such as ejecta from AGB or T Tauri systems and debris disks around young main sequence stars) can be established, assuming individual grain trajectories and velocities are known prior to detection. Such large ISPs should be able to penetrate deeply into the solar system without being stopped by the interplanetary magnetic field [3] and could potentially be detected at the Earth. Detection of large ISPs at the Earth has already been claimed based on data from the Advanced Meteor Orbit Radar (AMOR) operating in New Zealand [4].

**Equipment:** The Canadian Meteor Orbit Radar (CMOR) has been in routine operation since 2002 near 43N, 81W. This 6 kW interferometric automated radar operates at 29.85 MHz and records atmospheric trajectories and velocities for ~2500 meteoroids per day [5], [6]. The typical meteoroid mass detected by CMOR is near 10 μg, corresponding to particle sizes of order 100 μm. The beam coverage for CMOR is essentially all-sky, with 3 dB sensitivity contours located 60 degrees from the zenith. CMOR has a typical atmospheric collecting area of 200-300 $km^2$ for a given radiant direction. Meteoroid velocity is computed based on time-of-flight measurements made at two outlying stations; typical errors have previously been found to be of order 10% of the measured speed. Simulations [6] imply this error should be reducible by a factor of 2 – 3, suggesting further optimization of the existing signal analysis algorithms are warranted. Path orientation is dependent on both accurate measurement of the time-of-flight delays ($t_1$-$t_0$ and $t_2$-$t_0$ as in the figure) between different specular points along the trail as measured at the outlying stations (relative to the main station) and interferometric determination of echo location from the main radar station. Typical interferometric errors for high signal:noise ratio echoes are of order one degree.

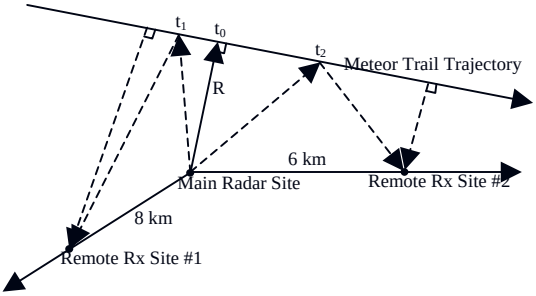


Figure 1.

**Analysis and Results:** A preliminary examination of potential very large ISPs detected by CMOR [7] produced only a handful (40) of possible detections from our initial population of more than $10^6$ orbits. The primary limitation of this earlier work was a 2σ selection criterion, i.e. only echoes whose heliocentric orbits were more than 2σ above the hyperbolic threshold were examined. In practice, this produced a cutoff for events with heliocentric speeds greater than 55 km/s at the Earth. Here we extend this earlier analysis to the 1σ case and examine the large number of hyperbolic meteoroids having heliocentric velocities below 48 km/s at 1 AU. We have further improved our time-of-flight detection algorithm producing higher precision velocity measurements. We will present results of this investigation examining the fraction of unbound orbits at the 1σ level as a function of ecliptic coordinates to establish the nature of the hyperbolic meteoroids (solar system or possible true interstellar). Earlier results from the AMOR system have also suggested a discrete southern hemisphere interstellar meteoroid stream source [4] at smaller masses than CMOR detects. We will similarly examine northern hemisphere data to search for such discrete sources at the larger particle sizes detected by CMOR.

**References:** [1] Gruen E. and Landgraf, M. (2000) *JGR, 105*, 10291–10297. [2] Frisch et al. (1999) ApJ., *525*, 492-516. [3] Landgraf, M. et al.. (2003) *JGR, 108*, LIS 7-1 [4] Baggaley, W.J. (2000) *JGR, 105*, 10353-10361. [5] Webster, A.R. et al. (2004) Atmos. Chem. Phys. Discuss., 4, 1181-1201. [6] Jones, J. et al. (2005) Planet. Sp. Sci., 53, 413-421. [7] Weryk, R.J. and Brown, P. (2005), Earth, Moon and Planets, accepted.

**WILD 2 OBSERVATIONS BY STARDUST** D. E. Brownlee, Department of Astronomy 351580, University of Washington, Seattle, WA, 98915 (brownlee@astro.washington.edu)

**Introduction:** The Stardust comet sample return mission successfully made a close flyby of comet Wild 2 on January 2, 2004. The flyby provided a close-up view of a 4.5 km diameter Jupiter family comet that is an active source of interplanetary dust. The mission provides both detailed information on ejected particles as well as information on the way in which comets eject particulates. During the flyby the spacecraft passed 234 km from the surface and onboard meteoroid sensors indicated that the fluence of impacting particles exceeded the primary mission goal for collection of more than 500 particles with diameters >15μm. In addition to meeting this goal, Stardust also made dust flux measurements with its acoustic and PVDF impact sensors (DFMI - Dust Flux Monitor Instrument), it measured mass spectra of impacting particles with its mass spectrometer (CIDA - Cometary and Interstellar Dust Analyzer) and took high resolution images with its optical navigation camera, an instrument whose primary function was to provide navigation data.

**Dust measurements:** The results from the dust impact and mass spectrometry measurements are reported elsewhere [1-4] and will also be elaborated in other presentations at this meeting.

**Dust collection and analysis:** The DFMI data indicate that thousands of analyzable particles impacted the Stardust's collector. About 85% of these particles were collected in low density silica aerogel designed to capture comet dust particles at the encounter speed of 6.1 km/s. About 15 % of the particles impacted aluminum foil that covered the aerogel support grid. The craters in foil can be analyzed for projectile residue and they can be used to directly determine the particle size distribution. The crater size distribution can be compared with the DFMA results and can also be used to calibrate the aerogel impacts.

When the collected samples are returned to Earth on January 15, 2006, a small portion of the particles will be studied during a 6 month preliminary analysis period by an international team of researchers. The primary goals of this initial investigation will be A) general characterization of the nature and state of preservation of the samples to provide information for the allocation and most efficient analysis of the samples, B) determine if the Wild 2 samples are similar or distinct from known types of material found in meteorites and interplanetary dust, and C) estimate the ratio of pre-solar to nebular components using criteria that are currently used for meteorites and IDPs.

**Encounter images:** The flyby occurred on the sunward side on the comet and the camera took 72 images over a full range of phase angles, providing stereo images of the entire sunlit hemisphere. The closest images have a scale of 14 m/pixel and the exposures were toggled between 10 ms and 100 ms, providing excellent images of the nucleus as well as the much fainter dust jets. A spectacular result from the imaging was the large number of highly collimated dust jets [5]. Due to the strong angular dependence of scattering, the jets were best seen at low phase angles. It was expected that one or two jets would be observed but 22 were detected. The high collimation of the Wild 2 jets is similar to those seen on Borrelly and, as suggested for Borrelly [6], their surface vents may be supersonic. The large number of jets, their small source regions, and the fact that almost the entire surface of Wild 2 is covered with depressions, suggests that the jets are short lived and occur, at various times, over most of the nucleus surface. The small size of the jet sources presumably produces an environment where weak aggregate comet particles can be comminuted by collisions that result from shear and differential acceleration. During the flyby, it appears that the majority of the jets originated from equatorial regions of the slightly oblate body. No jets were seen to originate from the sunlit polar region, perhaps an indication that this heated region has been, at least temporarily, depleted in volatiles in near-surface regions. Wild 2 had two jets emanating from the dark side implying that the sources of these regions remain active for an appreciable fraction of the spin period.

The surface of Wild 2 is appreciably different from the four other cometary nuclei that have be imaged- Halley, Borrelly and Temple 1. Temple appears to be covered with impact craters and presumably retains a significant of its surface that was exposed in the Kuiper belt. The remarkably complex and rough surface of Wild 2 is different from the other three comets, probably because of prolonged evolution in the inner solar system.

[1] Green S. F., et al (2004) JGR 109, 12, E12S04. [2] Clark B. C. et al. JGR 109, 12, E12S.03. [3] Tuzzolino A. J., et al. (2004) Science 304, 1776-1780. [4] Kissel, J(2004) Science 304, 1774-1776. [5] Sekanina Z., (2004) Science 304, 1769-1774. [6] Yelle, R.V. (2004) Icarus 167, 30-36.

**AN INTERNAL WATER OCEAN ON LARGE EARLY EDGEWORTH-KUIPER OBJECTS AND OBSERVATIONAL PROPERTIES OF SOME COMETS** V. V. Busarev, Sternberg State Astronomical Institute, Moscow University, Universitetskij pr., 13, Moscow 119992, Russian Federation, e-mail: busarev@sai.msu.ru

We have shown a possibility of a water ocean formation in the early Edgeworth-Kuiper objects (EKOs) [1]. A study of the most reliable data on matter content of the known comets, interplanetary dust particles, carbonaceous chondrites and utilization of the model distributions of the physico-chemical parameters of the matter in the solar proto-planetary disk allows to estimate an initial content of the short-lived $Al^{26}$ radionuclide in EKOs materials. A thermal balance calculation for the large bodies ($R$>100 km) shows that the quantity of heat discharged due to $Al^{26}$ decay in some first millions of years of their existence was sufficient to fully melt the water ice being in up to 30% proportion of their mass. An additional mechanism of EKOs' material heating up was probably a process of heat discharge under intensive collisional events in the mentioned and subsequent time. From analytical estimations [1] we have found that the water ocean might have been in a liquid state (at temperatures ~3-7°C) in EKOs' interiors for ~$10^7$ yr before complete freezing. This time was enough for the silicate fully sedimentation and serpentinisation, the silicate core formation (up to 0.5-0.6$R$ of the bodies) and for the dissolution or floating of the main part of organics to the upper water boundary [2]. The proposed model of EKOs' initial thermal evolution agrees well with available observational data on the bodies. Additionally, it makes possible to predict the physico-chemical properties of some new comets or to explain those of the known.

The comets could come from Kuiper belt as debris of differentiated EKOs (e. g., [3]) and may be distinguished by a large content of organic matter or dust as compared to the other comets. However, some of them are probably among observed dusty comets such as 21P Giacobini-Zinner, C/1987 P1 Bradfield, C/1988 A1 Liller and so on (e. g., [4]).

**References:** [1] Busarev V. V. et al. (2003) *EM&P, 92*, 345-357). [2] Busarev V. V. et al. (2005) *LPSC 36th*, abs. #1074. [3] Ipatov S. I., Mather J. C. (2003) *EM&P, 92*, 89-98. [4] Kiselev et al. (2000), P&SS, 48, 1005-1009.

**THE METEOROID ENVIRONMENT: SHOWER AND SPORADIC METEORS.** M. D. Campbell-Brown[1] and P. G. Brown[2], [1]University of Western Ontario, Department of Physics and Astronomy, London ON N6A 3K7, Canada, Margaret.Campbell@uwo.ca, [2] University of Western Ontario, Department of Physics and Astronomy, London ON N6A 3K7, Canada, pbrown@uwo.ca.

**Introduction:** Interplanetary particles larger than $10^{-13}$ kg (3 μm) create significant light and ionization when colliding with the atmosphere of the Earth. This provides a way to study the larger component of the interplanetary dust complex, since the collecting area of the Earth's atmosphere is large and the meteors resulting from these impacts are easily recorded with optical cameras and radars. Particles in this size range are generally too large to be captured in dust detectors, and are almost impossible to detect remotely. Meteoroids are generally divided into two broad categories: shower meteors, which come from narrow radiants and occur over a limited range of the Earth's orbit every year, and sporadic meteors, which are always active and come from diffuse radiants. Recent advances in observing technology, particularly in automated data analysis, have produced great advances in the understanding of meteoroid distribution at 1 AU.

**Shower meteors:** Many meteor showers have been linked with a parent object, most often a comet, though a few are linked with asteroids. The meteoroids generally have a very similar orbit to their parent body, and are thought to be relatively recent (<10 000 years) ejecta from the parent. Debris which is older loses coherence due to planetary perturbations and becomes part of the dust background. Their speeds and radiants are very similar, and tracing back their orbits can reveal the parent body. The recent rise in the discovery rate for near-Earth asteroids has also led to a resurgence in the investigation of potential asteroid – meteoroid stream associations (as in the case of the Quadrantids [1]). Recently, even the ejection age of streams has become constrained (extensively modeled for the Leonids [2]). This is now making it possible to use meteoroid stream activity as a proxy to constrain dust ejection models from comets, measure older active periods and past orbital behaviour of comets. Major showers, such as the Geminids, can nearly double the meteoroid flux at the Earth during their peaks; minor showers may only be visible after carefully subtracting the background activity. Some showers return year after year with similar activity levels; others may show outbursts in some years and even disappear in others. The major nighttime showers have been extensively studied with optical methods, but minor showers and daytime showers are much less understood. Maximum shower activity, averaged over five years of radar data from the Canadian Meteor Orbit Radar (CMOR) in Tavistock, Ontario, Canada), is shown in Figure 1, with the major showers marked.

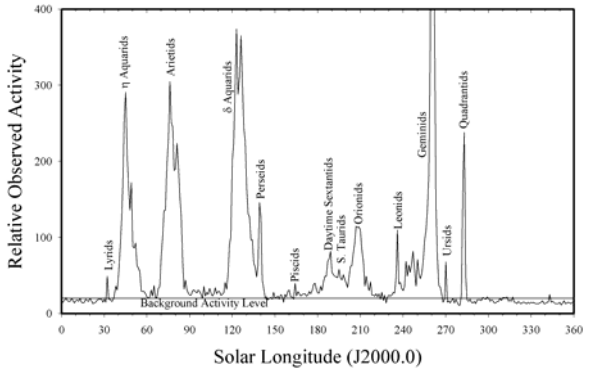


Figure 1. Maximum shower activity per degree of solar longitude; the data represents the average of five years of radar data

**Sporadic meteors:** Sporadic meteors are, by definition, those that do not belong to a recognized shower. They come from a few broad radiants which have constant positions relative to the sun. The most active sources are the helion and antihelion sources, which are centered near the solar and antisolar points; these and the apex source were first found by Hawkins [3], in a radio survey. The fastest sporadic meteors are associated with the apex source, which may be divided into a northern and a southern component, centered on the direction of the Earth's motion. The remainder of the sporadic meteors are concentrated approximately 60 degrees above and below the ecliptic, in the direction of the Earth's motion: these are the north and south toroidal sources (see [4] and [5]). Recent meteor patrol radar observations show the position and annual variation of these sources with unprecedented accuracy, and agree well with previous observations of the variation of the helion and antihelion sources [6]. A sample of CMOR sporadic data is shown in Figure 2, for April 10, 2004. The plot is in heliocentric coordinates, with the apex at the origin and the sun at +90 degrees. Sporadic meteors appear to have a longer dynamical history after separation from their parent body than shower meteors, but most appear to originate from short-period comets. Orbits of sporadic meteors have been studied extensively using radar [7]. Sporadic meteors are by far the dominant component of the meteoroid flux at the Earth, and become more dominant at smaller sizes. Because of the diffuse nature of the sporadic sources, they have been much less studied than shower meteors.

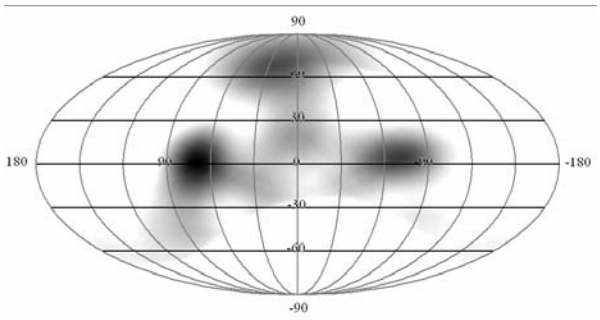


Figure 2: Heliocentric plot of sporadic radiants for April 10, 2004, as seen by CMOR, using an image resolution of 15 degrees. The apex of the Earth's way is at the origin, and the sun at +90 degrees. The north toroidal, north apex, helion and antihelion sources are clearly visible.

**References:**

[1] Jenniskens P., Marsden B.G., 2003, IAU Circ. 8252, 2.
[2] Lyytinen E.J., van Flandern T., 2000, EM&P 82, 149.
[3] Hawkins G. S., 1956, MNRAS 116, 92—104.
[4] Elford W. G., Hawkins G. S., 1964, Smithsonian. Astrophys. Obs. research rept no. 9.
[5] Jones J., Brown P., 1993, MNRAS 265, 524—532.
[6] Poole L.M.G., 1997, MNRAS 290, 245—259.
[7] Galligan D.P., Baggaley W.J., 2005, MNRAS 359, 551—560.

**NANOMETRE SCALE FILMS AS DUST DETECTORS.** J. D. Carpenter[1], T. J. Stevenson[2], G. W. Fraser[3] and A. Kearsley[4], [1,2,3]Space Research Centre, Department of Physics and Astronomy, University of Leicester, University Road, Leicester, LE1 7RH, UK, [1]jdc13@star.le.ac.uk, [2]tst@star.le.ac.uk, [3]gwf@star.le.ac.uk, [2]Natural History Museum, Cromwell Road, London, SW7 5BD, UK, A.Kearsley@nhm.ac.uk.

**Introduction and Background:** The exposure of 60nm thick aluminium films on the International Space Station (ISS) to assess the effects of the ISS environment on filmed microchannel plate (MCP) optics for the LOBSTER-ISS X-ray telescope [1] has resulted in the serendipitous discovery of nanometre scale dust and debris impactors. The inferred flux of this combined population is approximately $6m^{-2}s^{-1}$ [2]. These aluminium films are supported by the array of 12.5µm diameter MCP microchannels, which have a sensitivity almost two orders of magnitude greater than previously exposed foil experiments and are sensitive to impacts by dust particles with diameters of tens of nanometres.

**New Impact Site Analyses:** Since the discovery of this new population, work has been ongoing to analyse detailed impact morphologies on the films [3] and to determine the composition of the remaining trace residues through a combination of energy dispersive X-ray spectroscopy (EDXS) and secondary ion mass spectroscopy (SIMS). Such analyses can be used to refine impactor size estimates, sepatate different impactor populations and differentiate between natural dust and man-made debris impacts.

**Future Passive Detector Exposures:** Future thin film exposures, using films of varying thicknesses and pointing directions, and with an optimised location on the ISS are required, as the original ISS exposure was not optimised as a dust detection experiment. The exposed film surfaces need not be large. Analysis of the ISS exposed films indicates approximately one impact per minute for a $1cm^2$ surface area assuming that the density of impact features observed on the previously exposed films is characteristic of the flux in this size regime and is not dominated by a single event.

**Development of an Active Detector:** Such passive experiments are limited to retrievable samples in low Earth orbit. This environment is not ideal, particularly for the detection of very small particles, which are, in general, dominated by debris [4]. We are developing an active detector based on the thin film technology and utilising solid state detector readout solutions. Such a detector will use off the shelf devices, will be small, low in mass and suitable as an add-on to any spacecraft. It could therefore provide detailed data on nanonmetre scale dust populations throughout the Solar System.

**References:**

[1] Fraser, G. W. and 30 other authors (2002) *Proc. SPIE*, 4497, 115-126.

[2] Carpenter J. D., Stevenson T. S., Fraser G. W., Lapington J. S., Brandt D. (2005) *JGR., 110,* E05013, doi:10.1029/2004JE002392.

[3] Carpenter J. D., Fraser G. W., Stevenson T. J. (2005) *Proc. 4th European conference on Space Debris,* Darmstadt, Germany, In press.

[4] McDonnell J. A. M. (2001) in "Interplanetary Dust", edited by E. Grun, 163-261, Springer, London and Berlin.

**COMPOSITIONAL STREAMING AND PARTICLE FRAGMENTATION AT COMETS 1P/HALLEY AND 81P/WILD 2.** B.C. Clark, Lockheed Martin, POB 179, MS S-8000, Denver, CO 80201. benton.c.clark@LMCO.com

**Introduction:** The flyby of comet Wild 2 by the Stardust spacecraft revealed strong particle number density heterogeneities in the coma, while the Halley flyby missions showed that the particles in that cometary coma exhibit not only a great range in physical size, but also a range of compositions, including mixed particles and several apparent varieties of organic-rich materials. In this study, advantage is taken of the data from the Particle Impact Analyzer (PIA) on the Giotto spacecraft to provide a new classification of particle compositions in the coma of comet Halley. The time sequences of specific classes of particles are reexamined to evaluate potential additional evidence for spatial concentrations reflecting fragmentation and/or unique source regions, and compared with a model developed to characterize fragmentation patterns in the coma of Wild 2.

**Data:** Over 3000 TOS-MS spectra were obtained for elemental composition of Halley particulates by the PIA instrument. Each was time-tagged to an accuracy of 118 ms, corresponding to a distance traveled of 8 km. Over 9000 particles were analyzed for size by the Dust Flux Monitor Instrument (DFMI) on the Stardust mission, with a time resolution of 100 ms, or a spatial resolution element of 0.6 km. In both cases, the spacecraft flyby velocity was sufficiently higher than the cometocentric dust outflow speeds that the flux measurement can be interpreted directly in terms of number density of particle concentration. However, for PIA data not all events were transmitted.

**Approach:** Dust flux measurements in the Wild 2 coma have been recently analyzed in terms of a fragmentation model [1] and fragmentation interpretations [1, 2, 3]. Cluster sizes have been estimated from the model in terms of cluster radius and minimum mass content [1]. Similar metrics are now applied to apparent clusters in selected portions of the Halley coma, based upon specific compositional classes as determined from the PIA analyses. The classification scheme adopted here [4] utilizes a key element decision tree, with simple branching, building upon the initial compositional groups identified previously from PIA and PUMA data [5, 6, 1]. The first major branch in the trunk is for C, with immediate yes/no criteria for Si on both the C and no-C branches. These may be loosely interpreted as mineral and organic branches, and the four subsequent branches lead to silicates, non-silicate minerals (e.g., sulfides, oxides), organics, and Mixed particles containing C, Si, Mg and O (presumably, both carbonaceous and silicate matter). Subsequent branches result in 23 distinct classifications. Certain classifications can degenerate into other classes if one peak is missing, as can be the case for minor elements. Most of the classes are robust to criteria which provide independent methods of assessing their uniqueness.

**Results:** Although the statistical significance is marginal, it is found for example that Mixed particle encounter frequency is highly variable on the 3 s timescale (200 km), with evidence for 5 to 8 major apparent clustering's over a distance of 14,000 km in the coma. Even for this single particle class, variations in counts are significantly deviant from any simple Poisson distribution and the inverse-square law with distance from the nucleus is not strictly followed.

Numerous possible clusters are examined, for a range of grouped and ungrouped classes of particles. In many cases, there is correspondence in occurrence rate between members of different classifications, indicating a conglomerate source region, whether on the cometary surface or released as a large aggregate. In some cases, however, there is evidence of disparity between the classes of particles, with one or more members predominant and one or more members sparse. Correlations between types may be indicative of intrinsic associations of different types of cometary constituents, or possible undetected degeneracy's in the classification scheme.

**Applications:** The "ground truth" that the analyses of samples returned by Stardust should be helpful in refining the PIA and PUMA results, and relating the compositions of those portions of the two comae, Halley and Wild 2.

The refined analyses of these Halley results will be the only method available for ascertaining the similarities and differences in the compositional makeup of the particulate populations of comets Halley and Wild 2. In view of the loss of the CONTOUR comparative cometology mission, these data assume special significance.

**References:** [1] Clark et al. (2004), *JGR 109 : E12S03.* [2] Green et al. (2004), *JGR 109 : E12S43.* [3] Sekanina et al., *Science (2004) 304 : 1769-74.* [4] B.C. Clark and L. W. Mason (1991), Giotto/PIA Data Set, internally published. [5] Clark et al. (1987) *Astron. Astrophys. 187: 779-784.* [6] Fomenkova et al. (1994) *GCA., 58,* 4503-4512.

**BEHAVIOR OF CHARGED DUST IN PLASMA AND PHOTOELECTRON SHEATHS.** J. E. Colwell[1] , M. Horányi[1], S. Robertson[2], and P. Wheeler[2], [1]Laboratory for Atmospheric and Space Physics, University of Colorado, Boulder CO 80309-0392, josh.colwell@lasp.colorado.edu, [2]Dept. of Physics, University of Colorado, Boulder CO 80309.

**Introduction:** Dust particles in the regoliths of planetary satellites, asteroids, and ring particles can become charged due to photoemission from solar ultraviolet photons, solar wind currents, and in some case magnetospheric electrons. These currents produce a plasma sheath over the nighttime surface and a photoelectron layer over the daytime surface. Lunar electrostatic dust dynamics have been proposed for several observed dust phenomena [1-6]. Similar phenomena may play a role in the spokes of Saturn's rings [7, 8] and in the formation of smooth deposits in the floors of some craters on the asteroid Eros as observed by the NEAR-Shoemaker spacecraft [9].

**Observations:** Observations from the lunar surface by several of the Surveyor landers revealed a horizon glow over the western horizon shortly after sunset [3, 4, Figure 1].

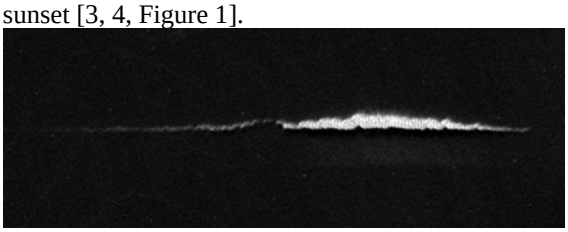

Figure 1: Observation of the Western horizon by the Surveyor 7 spacecraft shortly after sunset showing horizon glow. The glow is sunlight scattered by dust particles launched off the lunar surface by electrostatic forces.

The Lunar Ejecta and Meteorites Experiment (LEAM) detected increased signals near sunset and sunrise that have been interpreted as lunar dust particles moving over the surface [1, 2]. An analysis of the geometry of these images and the calculated levitation heights and trajectories for charged dust suggest that these observed dust particles are tens to hundreds of meters above the lunar surface. While they may be levitating or partially suspended, this may not be required to explain the observations of lunar horizon glow and the impacts detected by LEAM.

The NEAR-Shoemaker spacecraft observed smooth flat deposits, called ponds, in the floors of medium-sized craters. Observations are consistent with these deposits consisting of dust particles though they cannot rule out cm-sized particles. These ponds are in topographic lows that are therefore also regions of changing illumination and shadowing over the course of an Eros day. In addition, regolith (possibly dusty) aprons were observed adjacent to some large boulders and ejecta blocks on the surface of the asteroid.

**Simulations:** We simulate the trajectories of charged dust particles lifted off a dusty regolith, including gravitational and electrostatic forces as well as time-dependent charging of the grains. These simulations show a tendency for dust to accumulate in shadowed regions, suggesting that this charged dust transport may play a role in the dust deposits seen in craters and adjacent to large boulders on Eros. Particles in some conditions may be stably levitated over the surface with the electric force balancing gravity. We find that the typical stable levitation heights are much higher than previously assumed for most particles small enough to be levitated (Figure 2). Dust responsible for the lunar horizon glow (Figure 1) may be tens or hundreds of meters above the surface, rather than hovering at the Debye scale height of ~ 1 m above the surface.

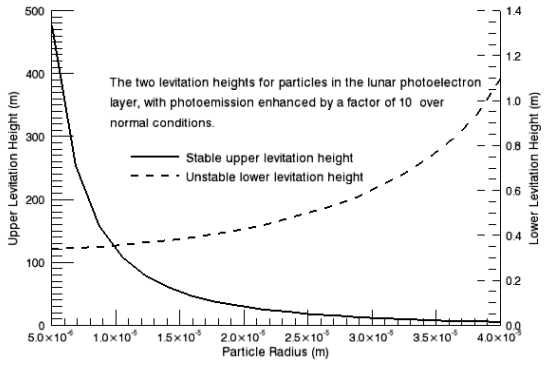


Figure 2: Calculated levitation heights for charged dust in the lunar photoelectron layer. The stable levitation height (solid line) is tens of meters for all particles except those close to the largest particle that can be suspended by the electric field.

On Eros we find levitation possible for particles smaller than 1 μm at heights of tens to hundreds of meters. Whether particles levitate or not, there is a net transport of dust into shadowed regions where there is no surface photoemission and therefore no vertical electric field to counter gravity. The

timescale for dust transport on Eros through this mechanism is short enough to explain the Eros crater dust deposits, though the simulations do not reproduce the smooth distribution of dust in detail. Other processes such as impact-induced seismic shaking likely also play an important role.

**Experiments:** We have performed experiments on levitation and transport of charged dust in a plasma sheath as well as charging of dust in a photoelectron sheath. In experiments where a small region of dust on a surface is exposed to a plasma, non-conducting dust particles, such as lunar and Martian regolith simulants, spread horizontally when placed on a conducting surface. This spreading is due to the dust particles charging to a potential that is significantly different from that of the conducting surface. This generates an electric field with a horizontal component that transports the dust away from the initial pile. Conducting dust on a conducting surface, on the other hand, remains at the same potential as the surface and no transport is observed. Experiments where the dust is placed on a sloped surface produce the expected transport of dust down the gradient in gravitational potential energy.

**Summary:** Observational evidence from several surfaces in the solar system points to charged dust particles lifting off the surface. Electrostatic effects can facilitate the transport of dust down gravity gradients and into regions of different electrical properties, such as different surface materials or shadowed regions. Terminator crossings are associated with increased dust activity on the lunar surface, but dust observed above the lunar horizon travels to much higher altitudes than previously estimated.

**References:** [1] Berg, O. E., E. F. Richardson, J. W. Rhee, and S. Auer (1974) *GRL, 1*, 289-290. [2] Berg, O. E., H. Wolf, and J. Rhee (1976) *Interplanetary Dust and Zodiacal Light* (Springer-Verlag), 233-237. [3] Rennilson, J. J., and D. R. Criswell (1974) *Moon, 10*, 121-142. [4] McCoy, J. E., and D. R. Criswell (1973), *LPSC, 5*, 496-497. [5] Zook, H. A., and J. E. McCoy (1991), *GRL, 18*, 2117-2120. [6] Zook, H. A., A. E. Potter, and B. L. Cooper (1995), *LPSC, 26*, 1577-1578. [7] Goertz, C. K. (1989) *Rev. Geophys., 27*, 271-292.. [8] Nitter, T., O. Havnes, and F. Melandsø (1998) *JGR, 103*, 6605-6620. [9] Colwell, J. E., A. A. S. Gulbis, M. Horányi, S. Robertson (2005), *Icarus, 175*, 159-169.

**A SEARCH FOR METEOR SHOWER SIGNATURES IN THE LDEF IDE DATA.** W. J. Cooke[1] and H. A. McNamara[2], [1]Meteoroid Environment Office, Mail Code EV13, Marshall Space Flight Center, AL 35812 USA, william.j.cooke@nasa.gov, [2]Meteoroid Environment Office, Mail Code EV13, Marshall Space Flight Center, AL 35812 USA, heather.a.mcnamara@nasa.gov

**Introduction:** For 346 days after the deployment of the LDEF satellite on April 7, 1984, the tape recorder belonging to the Interplanetary Dust Experiment (IDE) stored information on over 15,000 impacts made by submicron and larger-size particles on its metal oxide silicon (MOS) detectors . These detectors were mounted on trays facing in six orthogonal directions - LDEF ram and trailing edge, the poles of the LDEF orbit (north and south), and radially inward (towards the Earth) and outward (towards space). The 13.1 second time resolution provided by the IDE electronics, combined with the high sensitivity of the MOS detectors and large collecting area (~ 1 sq. m) of the experiment, conclusively showed that the small particle environment at the LDEF altitude of 480 km was highly time-variable, with particle fluxes spanning over four orders of magnitude.

A large number of the 15,000 impacts recorded by IDE occurred in groups, which were of two types - the *spikes*, single, isolated events of high intensity and the *multiple orbit event sequences* (MOES), which were series of events separated in time by integer multiples of the LDEF orbital period. Even though the spikes were generally more intense, the MOES could be quite long-lived, some lasting for many days.

A previous paper by Cooke et al. [1] attributed the MOES to impacts by man-made debris particles in orbits intersecting that of LDEF. The 20 day longevity of one of these events – termed the *May Swarm* – led to the suggestion that the debris particles must be constantly replenished by their source, as the orbits of micron sized particles will rapidly decay under the influence of radiation pressure and other non-gravitational forces, entering Earth's atmosphere after only a few revolutions.

However, the date of onset of the May Swarm (May 22) and the long duration of this event may indicate a possible correlation with the annual Arietid meteor shower, which peaks around June 8. As this seemed to hold the promise of a less "artificial" explanation than a satellite or rocket body continuously "dribbling" debris , it was decided to take a fresh look at parts of the IDE data set in an attempt to detect meteor showers within the impact record.

**Analysis**: Three major annual showers – the daytime Arietids, the Perseids, and the Geminids were chosen for the initial search. A subset of the data, the impact record for the IDE space facing tray was extracted, as this set of detectors should sample the meteoroid environment with little contamination from orbital debris. The number of impacts on the tray facing radially down, towards Earth, was too small to be useful, as it was shielded by the Earth.

There was no shower signature detected for the Geminids; no impacts on the space tray occurred while it was exposed to the shower radiant. However, the Perseids showed a remarkably strong signature – 18 impacts on the 1 μm detectors occurred over the shower duration while the tray was exposed to the radiant, with only one occurring when it was not. Figure 1 shows the impact record, binned in 1 day intervals, for the 1 μm space-facing detectors from July 17 to August 24; Note the concentration of impacts about day 225 – August 11, near the time of the traditional Perseid peak.

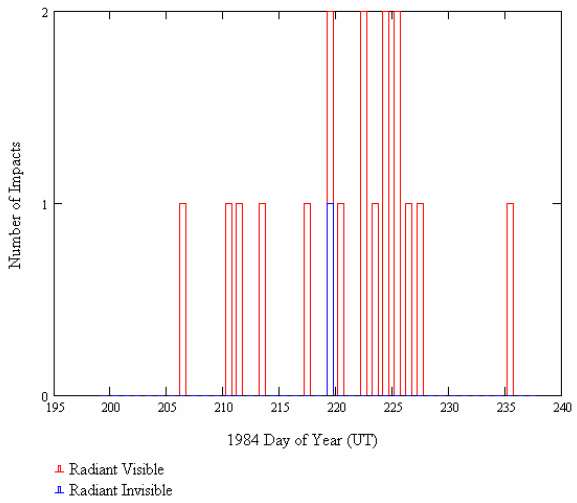


Figure 1. Impacts on IDE space facing 1 μm detectors from July 17 to August 24, 1984.

There is also a strong impact signature during the daytime Arietids (May 22 – July 8). However, the fact that this radiant is close to the Sun, being imbedded in the sporadic Helion source, and also the high likelihood that IDE observed significant numbers of β meteroids [2], make it difficult, if not impossible, to attribute any of these impacts to the Arietids with confidence.

Searches for other showers (Eta Aquarids and Orionids) were also conducted. The results of these, and

more details of the analyses will be presented, along with an examination of the possible causes for the "May Swarm."

**References:**

[1] Cooke W. J. et al. (1995) *LDEF 3rd Post-Retrieval Symposium*, 361-371.

[2] Cooke W. J. et al. *Advances in Space Research, 13*, 119-122.

**CONTINUOUS LARGE-AREA MICROMETEOROID FLUX MEASURING INSTRUMENT.** R. Corsaro[1], J.-C. Liou[2], F. Giovane[1], and P. Tsou[3], ([1]Naval Research Laboratory, Washington D. C. 20375, Corsaro@NRL.Navy.mil, [2]ESCG/ERC at NASA JSC, [3]NASA Jet Propulsion Laboratory).

**Introduction:** An instrument capable of continuously measuring the flux of micrometeoroids is described in this paper. The instrument can be utilized in interplanetary space or on planetary or satellite surfaces for future solar system exploration missions.

**Heritage:** Funded by NASA Planetary Instrument Definition and Development (PIDD) Program, an instrument was developed combining a conventional aerogel particle collector with a new acoustic system for detecting the time of each particle's arrival. This latter system, called PINDROP (Particle Impact Noise Detection and Ranging On autonomous Platforms) uses piezoelectric strain sensors to detect the time and location of each particle impact [1]. In addition, the signal rise time and the waveform of the signal can be used to estimate the impact speed. Knowing the time and speed of impact, combined with direction information from the particle track in the aerogel (measured on retrieval), permits a possible determination of the orbit of the impactor. A dynamical link from the collected sample to its parent object may be established. This highly successful instrument development effort has led to a 10 square meter system currently under development called LAD-C (Large Area Debris Collector), which is scheduled for deployment on the ISS in 2007 [2].

The PINDROP acoustic detection system component can also be used without aerogel in cases where retrieval is not practical. On man-made structures, the sensors can be applied directly to hard surfaces as well as thin fabric to form a large sensing array. This has been demonstrated in laboratory tests on various materials including, for example, the outer layer of a conventional thermal blanket. Using telemetry, the instrument then can continuously monitor particle impact flux, as well as platform noise for diagnostic purposes.

The previous systems have many applications, particularly on near-Earth satellites and platforms. However they have some limitations for interplanetary applications. In particular, when used to monitor infrequent large particles, the large arrays required will involve using a very large number of sensors. Additionally the sensors have temperature limitations that make them unsuitable in very warm environments.

**New Capability:** A variation on this instrument has been proposed for a large-area solar sail deployment. It consists of thin sail-like polymer film supported by a frame containing associated surface motion detectors. Micro-particles impacting the film generate surface vibrations that can be detected by displacement sensors located near the supports.

The impacting particle generates surface motion in the film predominately at the normal modes of the structure. As such, it behaves much like a drum. This has two benefits: the motions induced are relatively large due to the modal response of the surface, and only a few sensors are required to monitor this motion. Because of the relatively low frequency of these responses, the entire surface can be monitored with relatively few sensors.

**Status:** The optimum sensor type to detect film vibrations caused by particle impacts has been determined to be a surface-normal fiber optic displacement sensor. Sensors of this type developed for other applications at NRL have very high sensitivity to displacement (nominally 1 Angstrom), operate over a wide range of temperatures (to 1000°C) and are relatively insensitive to radiation.

The feasibility of this system was demonstrated using a hypervelocity impact range at NASA JSC [3]. A fiber optic displacement sensor was attached to the frame supporting a test section of a film (intended for a solar sail), and the motion of the film was monitored during an impact with a hypervelocity particle. The strong vibrations induced in the film following impact were easily detected by this sensor.

**Applications:** Potential applications for this instrument include (1) characterization of particle environment near and on the surfaces of the Moon, Mars, and other planets or satellites and (2) monitoring impacts on large-scale structures for future exploration missions. For example, the condition of a sail-like film can be continuously monitored since the modal frequencies depend on tension. Hence the device is a low-cost low-mass addition to any sail-like structure, such as the proposed Solar Sail platform.

**References:**

[1] New Scientist, (28 Aug 2004, page 20) (staff writer) [2] R. Corsaro, F. Giovane, P. Tsou, J.-C. Liou, D., Buzasi, B. Gustafson, (2004) *Orbital Debris Quarterly News* Vol. 8, Issue 3, 3-4. [3] J.-C. Liou, E. Christiansen, R. Corsaro, F. Giovane, and E. Stansbery (2005) *Orbital Debris Quarterly News*, Vol. 9, Issue 1, 6-7..

**UPGRADE OF METEOROID MODEL TO PREDICT FLUXES ON SPACECRAFT IN THE SOLAR SYSTEM AND NEAR EARTH.** V. Dikarev[1,2], E. Grűn[1,3], W. J. Baggaley[4], D. P. Galligan[4,5], R. Jehn[6], M. Landgraf[6], [1]Max-Planck-Institut fűr Kernphysik, Heidelberg, Germany, [2]Astronomical Institute of St. Petersburg University, Russia, [3]Hawaii Institute of Geophysics and Planetology, University of Hawaii, USA, [4]University of Canterbury at Christchurch, New Zealand, [5]Currently at Defence Technology Agency, Devenport, New Zealand, [6]ESA/ESOC, Darmstadt, Germany.

We present some aspects of the new interplanetary meteoroid model developed to predict fluxes on spacecraft in the Solar system and near Earth. The model is distinguished from the previous work due to the new data incorporated, new design of the meteoroid populations whose orbital distributions are now constructed using approximate theories of the orbital evolution, and an outstanding quality of fit to observations. With the new experience from modeling the interplanetary dust cloud on the large scale, we come up with some recommendations for the future development of scientific and engineering models of meteoroid environment.

**CALORIMETRIC AEROGEL PERFORMANCE AT INTERSTELLAR DUST VELOCITIES.** G. D. Dominguez[1], A. J. Westphal[1], S. M. Jones[2], M. L. F. Phillips[3] and M. Schrier[3], [1]Space Sciences Laboratory, U. C. Berkeley, Berkeley, CA 94720-7450, [2]Jet Propulsion Laboratory, Pasadena, CA 91109, [3]Pleasanton Ridge Research Corporation, 27468 Hayward Blvd, Hayward, CA 94542

**Introduction:** No contemporary interstellar dust particles have ever been identified and analyzed in the laboratory. The Stardust mission will return a few dozen small (~1 micron) interstellar dust grains in January 2006. Identification of these grains will be a major challenge, and is the focus of the Stardust@home project [1]. Analytical techniques available to study such small grains exist but are limited.

A large collecting power, of order several $m^2$-years, is required to collect large (several micron) interstellar dust grains[2]. Such a large array can probably be deployed most easily in low-earth orbit (LEO), but the ubiquitous orbital debris in LEO would present an huge background that would probably preclude the identification of IS dust using ordinary silicate aerogels.

We have recently developed a robust, monolithic, fluorescent "calorimetric" aerogel. The aerogel is silica doped with Gd and Tb, and is ordinarily not fluorescent. When heated the aerogel undergoes a permanent phase transformation to a brightly fluorescent phase. This phase transformation occurs even with the very brief thermal pulse associated with the capture of a hypervelocity particle. We have previously demonstrated that the integrated fluorescence intensity (S) is a function of the kinetic energy of the captured hypervelocity particle[2]. Such an aerogel could be used to collect orbital debris and extraterrestrial hypervelocity dust grains in low-earth orbit, and simultaneously passively record the kinetic energy of each hypervelocity impact. Since it is passive and requires no power or telemetry, an instrument composed of calorimetric aerogel would be intrinsically low-risk. It is also extremely simple --- all of the sophistication of the instrument is in the post-recovery terrestrial laboratory. Such a collector could also be used to capture and identify for the first time thousands of contemporary interstellar dust grains in LEO, and, depending on the collecting power, many large IS dust grains.

**Calibration:** Until recently, all of the calibrations of this calorimetric aerogel have been done at relatively low velocities (<6 km $sec^{-1}$) and with glass beads ($\rho$=2500 kg $m^{-3}$). Here we report measurements of the detector response at much larger velocities, characteristic of the speeds of the interstellar dust that is continuously streaming into the Solar System from the local interstellar medium. The detector was exposed to 10-12 and 18-22 km $sec^{-1}$ latex spheres (r~0.375 and 0.8 μm) using the 2 MV Van-de-Graaff accelerator in Heidelberg. We subsequently examined the calorimetric aerogel using a standard UV microscope at the Biological Imaging Facilities in Berkeley and found that there were fluorescent impact features in the exposed aerogel samples (Fig. 1). These fluorescent impact craters were then imaged and the integrated fluorescence signal was determined using techniques similar to those used in [2]. The dispersion in the signal for these particles corresponds to a velocity resolution of ~20%, similar to that of previous calibrations.

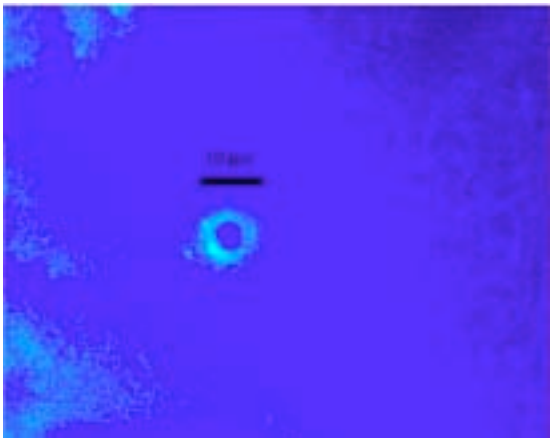

**Figure 1. Fluorescence image of latex sphere (r=0.375 - 0.8 microns) with impact velocity equal to 10-12 km/s. This image was taken at 20x magnification. The contrast has been enhanced for clarity.**

We have previously found that the response of this calorimetric aerogel can be described by a function of the form $S=Ar^a v^b$ with a=2.16 and b=1.8 [3]. These values imply that the calorimetric aerogel responds to the kinetic energy loss of the projectile near the surface of the aerogel. The results of our experiments with latex spheres with v> 10 km $sec^{-1}$ suggest that the response of the calorimetric aerogel is fundamentally different at higher velocities. This is evident in Fig. 2 where the response of our shots at Heidelberg is compared to the response of the lower velocity shots (v<6 km $sec^{-1}$). To directly compare

the two data sets, a correction factor was applied to the Heidelberg data to account for differences in magnification and lamp intensity between the two data sets. That the response is significantly higher than a naïve extrapolation from lower velocities predicts, suggests that the size threshold for interstellar particles could be quite small.

The Heidelberg data show that the response of calorimetric aerogel continues to increase as a function of velocity. Because the size of latex spheres at higher velocities (18-22 km sec $^{-1}$) was smaller (r~0.3 μm) than those at 10-12 km sec $^{-1}$ (r~0.8 μm), this effect is even more dramatic than it appears in Fig. 2. Future work with latex spheres velocities will be needed in order to determine the detailed response function of this calorimetric aerogel to hypervelocity dust with v>10 km km sec $^{-1}$.

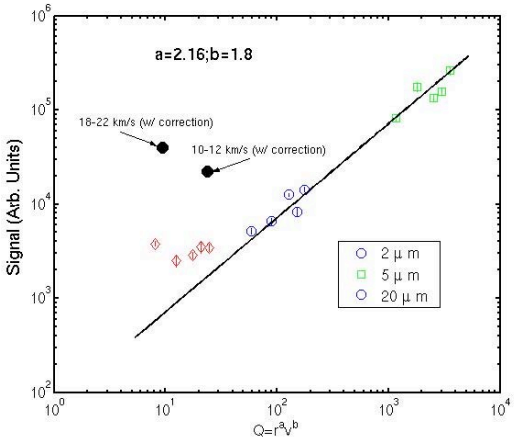


**Figure 2. Combined response function of calorimetric aerogel to both glass and latex spheres (black dots).**

**References:** [1] Westphal, A. J. et al. (2005) *LPS XXXVI*, Abstract #1908. [2] Dominguez, G., Westphal, A. J., Phillips, M. L. F., and Jones, S. M., (2003) Astrophys. J. 592, 631. [3] Dominguez, G. D. et al. (2005) in press; Dominguez, G. D., PhD Thesis, U. C. Berkeley (2005).

**Additional Information:** This work was supported by the NASA PIDDP program. We are grateful to Ralf Srama and Anna Mocker-Ahlreep for their generous support at Heidelberg.

**SIZE-FREQUENCY DISTRIBUTIONS OF DUST-SIZE DEBRIS FROM THE IMPACT DISRUPTION OF CHONDRITIC METEORITES.** D. D. Durda[1], G. J. Flynn[2], L. E. Sandel[3], and M. M. Strait[3]. [1]Southwest Research Institute, 1050 Walnut Street Suite 400 Boulder CO 80302 durda@boulder.swri.edu, [2] SUNY-Plattsburgh Plattsburgh NY 12901, [3]Alma College Alma MI 48801.

**Introduction:** In order to understand the collisional evolution of asteroids and interplanetary dust and to accurately model the infrared signature of small particles in our own Solar System and in other young planetary systems, we must address the fundamental problem of better understanding dust production from primary impact disruption events covering a wide range of sizes. At present, however, we understand well the size frequency distributions (SFDs) for collision fragments within only a couple orders of magnitude of the size scale of the original target body; for impact disruption events at all size scales we still know next to nothing (and in many cases identically nothing) about the primary production of fragments many orders of magnitude smaller than the original target body size. Thus, existing modeling results in these areas have tremendous uncertainties.

Laboratory-scale impact experiments can provide direct know edge of the SFDs of dust-size debris produced directly from the impact disruption of ~5-cm scale meteorite targets, roughly the size scale of the immediate parent bodies of zodiacal dust particles. Here, we report results of a set of impact disruption experiments involving chondritic meteorite samples, conducted at the NASA Ames Vertical Gun Range (AVGR). Preliminary results from these experiments were reported previously in [1].

**Impact Experiments:** Chondrite meteorites were impacted by small aluminum projectiles at speeds of about 5 km/s in order to examine the production of dust particles and the mechanics of fracture of real meteoritic materials under the impact regimes that presently exist in the main asteroid belt. The ~5 cm-scale targets were each suspended at the center of the AVGR impact chamber and surrounded with four passive dust 'detectors' consisting of thin aluminum foils (~7- and 13-μm thick, mounted in 35mm slide mounts, and 51-μm thick, taped across larger cutouts in the detector foam core backing) and rectangular blocks of aerogel (with dimensions of ~2×2×3 cm). Figure 1 shows one of the detectors in detail and in place in the impact chamber near one of the meteorite targets. The foils were thin enough that high-speed particles would penetrate, providing a size distribution of ejecta; particles captured intact in the aerogel were analyzed *in situ* for chemical composition [2,3]. Large fragments were collected from the chamber and weighed. The impacts were recorded by 500 fps video.

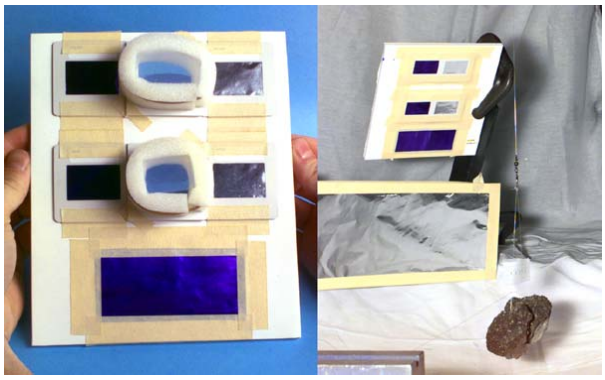

Figure 1. Passive particle detectors used in AVGR impact experiments to capture and measure the properties of dust-size debris. (Left) Detail showing the arrangement of foils and aerogel in a typical detector layout. ~7-, 13-, and 51-μm thick foils are set along the top, middle, and bottom rows, respectively, with blocks of aerogel set in foam holders between the foils. (Right) typical deployment of a detector near a meteorite target within the AVGR impact chamber.

**Foil Hole Data:** The foil hole sizes were measured via two independent methods. To cover the entire area of a particular foil (equal to the window size of a standard 35mm slide mount), the foil was scanned with Nikon slide scanners at 2700 dpi and at 4000 dpi. The resulting 3894×2592 pixel and 4000×5888 pixel images have a resolution of ~9.4 and ~6.3 μm/pixel, respectively. Figure 2 shows an example of one of the slide scanner foil images. Smaller, sample areas of some foils were surveyed with a microscope/video setup at a resolution of ~1.6 μm/pixel. The hole size distributions from the resulting scanner and microscope images were determined by analysis with the software package ImageJ from NIH.

**Preliminary Results:** Analysis of the foil image data is still underway. Results presented in [1], however, are illustrative of the more complete data sets that will be used to extend the SFDs of the fragments from the disruption of the meteorite samples down to dust-size particles.

As an example, Fig. 3 shows the size distribution of holes from the 7-μm thick foil from detector 3 of shot 011015 (the target for this shot was a 248.0 g sample of NWA620, an unclassified ordinary chondrite; the projectile was a ¼-in aluminum sphere impacting at 5.59 km/s), which was mounted 48 cm from

the target, roughly 240° in azimuth from the direction of the incoming projectile. The holes appear to represent comparatively low-speed ejecta and tend to lie at the bottom of stretched impact depressions in the foil (holes observed in other foils from other shots clearly resulted from high-speed particles, being cleanly punched and displaying surrounding, raised rims). The scanner image for this foil was tightly focused and the distributions measured from the scanner and microscope data are very similar.

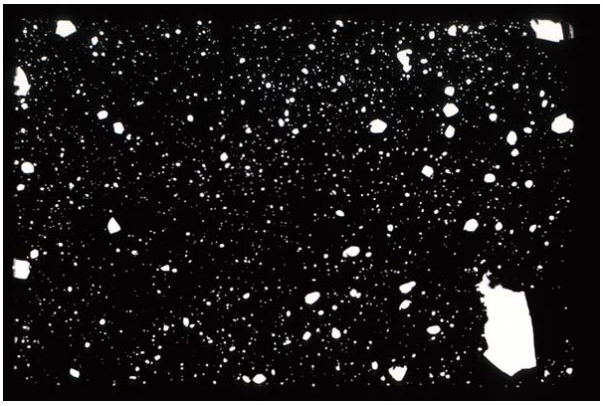

Figure 2. Slide scanner image of a 7-μm thick foil from detector 3 of shot 011015. The image resolution is 2700 dpi.

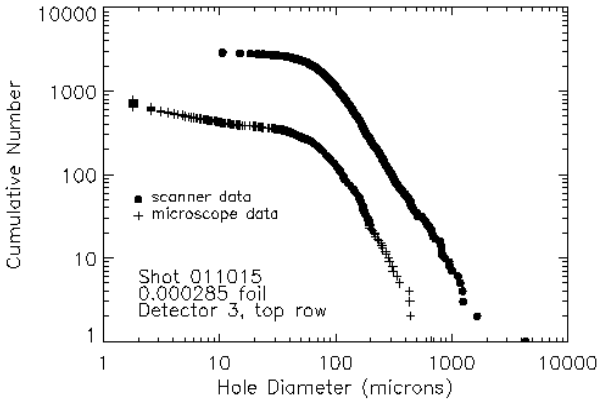


Figure 3. Size distribution of 'low-speed' holes from a 7-μm thick foil from detector 3 foil of shot 011015.

Similar data from the other foils from this and the other shots will be combined to extend the mass frequency distributions of mm- to cm-scale fragments down to dust-size particles. The foil/aerogel detectors were arranged to provide a broad sampling of the dust flux through area surrounding the meteorite targets; when properly normalized to the full 4π steradians surrounding the targets, the dust SFDs will provide very useful knowledge of the primary fragment SFDs to much smaller sizes than is conventionally measured in laboratory impact experiments.

**References:** [1] Durda D. D., Flynn G. J., Hart S. D., and Asphaug E. (2002) *LPS, XXXII*, abstract #1535. [2] Flynn G. J and Durda D. D. (2004) *Planet. Space Sci.*, **52**, 1129-1140. [3] Flynn G. J. et al. (1996) *LPS, XXVII*, 369.